World Journal of Engineering Research
Print ISSN: 2959-9865
Online ISSN: 2959-9873
DOI: https://doi.org/10.61784/wjer3123

PROCESSING-DEPENDENT WORK HARDENING AND AGEING RESPONSE OF AZ91, AJ63 AND AE44 MAGNESIUM ALLOYS

RuiJie Guo
Department of Materials, Imperial College London, South Kensington Campus, London SW7 2AZ, UK.

Abstract: Magnesium alloys are attractive lightweight structural materials, but their limited room-temperature hardness and deformation resistance require strengthening through heat treatment and plastic deformation. This study systematically compared the processing responses of three cast magnesium alloys, AZ91, AJ63 and AE44, under identical laboratory conditions. As-cast bars were subjected to solution treatment at 410 °C for 24 h, rolling deformation, ageing at 175 °C for 2-72 h, and combined solutionising-rolling-ageing routes. Vickers hardness was measured using a 2 kg load. Optical micrographs were used to relate hardness evolution to phase morphology and deformation behaviour. Solution treatment alone produced no statistically significant hardness increase in any alloy. AZ91 showed the strongest strengthening response: direct rolling produced hardness above 76 HV in the low-strain range, and the combined route of solutionising, 15% rolling and ageing for 18 h increased hardness to approximately 82.4 HV. AJ63 was highly sensitive to brittle cracking in the as-cast condition; effective work hardening was only obtained after solutionising, with hardness rising to approximately 62-63 HV after rolling and ageing. AE44 showed a weaker ageing response, but rolling continuously increased hardness to approximately 50-51 HV at around 13% strain. The results demonstrate strong composition-dependent processing behaviour. AZ91 benefits most from strain-assisted ageing, AJ63 requires solution treatment before rolling, and AE44 is better strengthened by controlled deformation than by solution treatment alone.
Keywords: Magnesium alloys; AZ91; AJ63; AE44; Solution treatment; Rolling deformation; Ageing hardening; Vickers hardness; Work hardening

1 INTRODUCTION

Magnesium alloys have attracted sustained attention as lightweight structural materials because of their low density, high specific strength and potential for reducing component weight in automotive, rail transport, aerospace and electronic applications [1-2]. Their wider use, however, remains restricted by relatively low hardness, limited room-temperature formability, rapid texture development during deformation and sensitivity to microstructural defects. These limitations make microstructure control through alloy design, heat treatment and deformation processing central to improving the performance of commercial magnesium alloys [3-4].

Hardening in magnesium alloys can arise from several mechanisms, including solid-solution strengthening, precipitation strengthening, grain-boundary strengthening and strain hardening. In Mg-Al based alloys, solution treatment can dissolve part of the beta-Mg17Al12 phase and produce a supersaturated matrix; subsequent ageing can generate precipitates that interact with dislocations [3, 5]. Plastic deformation introduces dislocations, twins and texture changes. When followed by ageing, deformation can also accelerate precipitation by supplying nucleation sites, giving a combined strain-ageing effect [6-7].

AZ91, AJ63 and AE44 provide a useful comparison because they contain different secondary phases. AZ91 is a Mg-Al-Zn alloy in which beta-Mg17Al12 is the dominant hardening phase. This phase can partly dissolve during solution treatment and reprecipitate during ageing [5]. AJ63 is a Mg-Al-Sr alloy containing Sr-rich intermetallic phases such as Al4Sr or (Al,Mg)4Sr, which can improve high-temperature stability but may also form brittle networks in the as-cast microstructure [8-9]. AE44 is a Mg-Al-rare-earth alloy that commonly contains thermally stable Al-RE intermetallics such as Al11RE3 and Al2RE. These phases are important for creep resistance and thermal stability, but they leave less aluminium available for conventional Mg-Al age hardening [10-12].

Although many studies have considered individual AZ, AJ or AE alloy systems, direct comparison under the same solutionising, rolling and ageing conditions is less common. To the best of the author's knowledge, this work provides a systematic comparison of the work-hardening and ageing responses of AZ91, AJ63 and AE44 under identical laboratory processing conditions, enabling a direct evaluation of composition-dependent deformation behaviour. The objectives were: (i) to quantify the effect of solution treatment on hardness; (ii) to compare rolling-induced work hardening and cracking sensitivity; and (iii) to identify suitable combined processing routes for each alloy.

2 MATERIALS AND METHODS

2.1 Materials and Experimental Design

Three commercial magnesium alloys, AZ91, AJ63 and AE44, were investigated. The alloys were supplied as as-cast bars. No prior heat treatment or deformation processing was reported before the experiments. The exact supplier, casting route and measured chemical composition were not available in the original dataset; therefore, the nominal compositions used for interpretation are listed in Table 1. For final journal submission, supplier information, bar dimensions, casting route and measured composition should be inserted if available.

Table 1 Nominal Compositions and Phase Characteristics of the Three Investigated Magnesium Alloys

Alloy	Nominal alloy system	Key alloying elements	Expected dominant secondary phases	Alloy
AZ91	Mg-Al-Zn	~9 wt.% Al, ~1 wt.% Zn	beta-Mg17Al12 and Al-containing precipitates	AZ91
AJ63	Mg-Al-Sr	~6 wt.% Al, ~3 wt.% Sr	Al-Sr intermetallics, including Al4Sr/(Al,Mg)4Sr and ternary Sr-containing phases	AJ63
AE44	Mg-Al-RE	~4 wt.% Al, ~4 wt.% rare earth elements	Thermally stable Al-RE phases, mainly Al11RE3 and Al2RE	AE44

2.2 Solution Treatment, Rolling Deformation and Ageing

Solution treatment was carried out at 410 °C for 24 h. Samples were heated in a furnace and then quenched in room-temperature water to retain the solutionised state. Some solutionised specimens were tested directly, while others were subjected to rolling and/or ageing. Because heating rate, water temperature, quench transfer time and cooling rate were not recorded, these parameters should be standardised in future work.

Rolling was performed on a laboratory rolling mill. The thickness reduction per pass was controlled between 1% and 20%, depending on alloy condition and cracking behaviour. After each pass, the sample thickness was measured and the next pass was carried out until the target strain was reached or visible surface cracking occurred. Rolling was treated as a unidirectional thickness-reduction process. For higher reproducibility, future work should report roll diameter, rolling speed, lubrication condition, rolling temperature and whether any inter-pass annealing was used.

Ageing treatment was conducted in an oil bath at 175 °C for 2-72 h. Both unrolled and rolled specimens were aged to evaluate individual ageing and combined strain-ageing effects. The combined route is referred to as solutionising + rolling + ageing when rolling followed solution treatment, and as cast rolling + ageing when deformation was applied directly to the as-cast sample.

2.3 Vickers Hardness Testing and Statistical Treatment

Vickers hardness was measured using a 2 kg load. Three parallel samples were used for each route, and ten indentations were taken per sample. The reported hardness values are expressed in HV. For the solution-treatment comparison, three sample-level values were available and were analysed as mean ± standard deviation. Welch's t-test was used to compare as-cast and solutionised conditions for each alloy. Because only averaged trend data were available for most rolling and ageing curves, full ANOVA across all strain and ageing conditions was not attempted. This is noted as a limitation of the present dataset.

2.4 Metallographic Observation

Optical micrographs were used to examine the as-cast, solutionised and aged microstructures. The available images show the morphology and distribution of secondary phases in AZ91, AJ63 and AE44. Each micrograph includes a scale bar of 500 μm. A complete journal submission should additionally report the observation plane, grinding and polishing procedure, etchant composition, etching time and optical microscope model.

2 RESULTS

3.1 Effect of Solution Treatment on Hardness

The hardness changes produced by solution treatment were small for all three alloys (Table 2). AZ91 decreased from 58.58 ± 1.53 HV in the as-cast state to 58.14 ± 1.40 HV after solutionising. AJ63 changed from 51.57 ± 3.25 HV to 50.73 ± 0.44 HV, while AE44 decreased from 44.30 ± 1.46 HV to 43.29 ± 0.30 HV. Welch's t-tests indicated that none of these differences was statistically significant at $p < 0.05$. Therefore, under the condition of 410 °C for 24 h, solution treatment alone did not provide measurable hardness strengthening.

3.2 Effect of Rolling Deformation on Hardness

Rolling deformation produced alloy-dependent hardness responses (Figure 1). For AZ91 rolled in the as-cast condition, hardness first increased and then decreased with increasing strain. The hardness reached approximately 76.5 HV at low-to-intermediate strain and then decreased to about 71.2 HV at 10% strain and 68.8 HV at 20% strain. This indicates that an optimum rolling strain exists for as-cast AZ91, beyond which cracking, phase fragmentation or recovery-related softening may offset strain hardening.

For solutionised AZ91, the hardness initially decreased and then increased with strain, suggesting that solution treatment altered the balance between softening by phase dissolution and hardening by dislocation accumulation. AJ63 behaved differently. Direct rolling of as-cast AJ63 caused a sharp hardness decrease from around 51-53 HV to approximately 40.9 HV at 1% strain and 35.9 HV at 5% strain, accompanied by visible cracking. After solution treatment, however, AJ63 showed normal work hardening: hardness increased to about 59.6 HV at 5% strain and approximately 62.1 HV at 8% strain. AE44 showed a mild initial decrease followed by continuous hardening, reaching approximately 50 HV at 13% as-cast rolling strain.

Table 2 Vickers Hardness Before and After Solution Treatment. P-Values Were Calculated Using Welch's T-Test from the Three Available Sample-Level Values

Alloy	Condition	Hardness (HV, mean ± SD)	n	p-value vs as-cast	Interpretation
AZ91	As-cast	58.58 ± 1.53	3	-	The change after solution treatment was not statistically significant.
AZ91	Solutionised	58.14 ± 1.40	3	0.731	
AJ63	As-cast	51.57 ± 3.25	3	-	The apparent change was not statistically significant; scatter in the as-cast samples was larger.
AJ63	Solutionised	50.73 ± 0.44	3	0.699	
AE44	As-cast	44.30 ± 1.46	3	-	The decrease after solution treatment was small and not statistically significant.
AE44	Solutionised	43.29 ± 0.30	3	0.354	

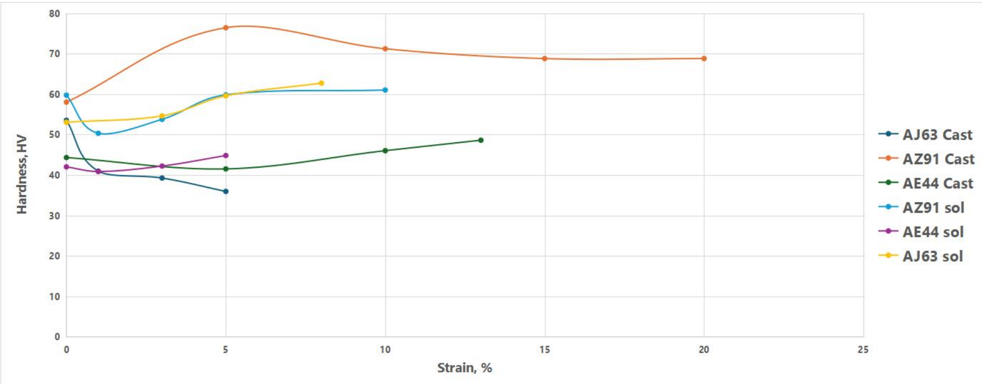

Figure 1 Vickers Hardness as a Function of Rolling Strain for As-Cast and Solutionised AZ91, AJ63 and AE44 Magnesium Alloys. The Curves Show Distinct Composition-Dependent Work-Hardening Behaviour

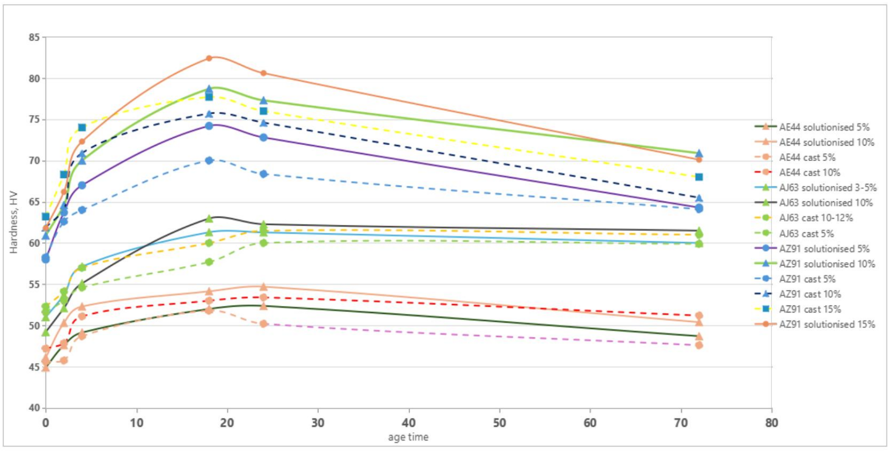

Figure 2 Vickers Hardness as a Function of Ageing Time and Heat Treatment Condition for Cast and Solutionised AZ91, AJ63 and AE44 Magnesium Alloys

3.3 Effect of Combined Solutionising, Rolling and Ageing

The combined processing routes showed the clearest improvement in AZ91 (Figure 2). After solution treatment, rolling at 15% strain and ageing at 175 °C for 18 h increased hardness to 82.4 HV. This value was higher than ageing alone (approximately 74.2 HV) and rolling alone (approximately 71.2 HV), indicating a synergistic effect between deformation-induced defects and subsequent precipitation.

For AJ63, the recommended route was solutionising followed by rolling at approximately 8-10% and ageing for 18 h. This produced hardness of approximately 63 HV, only slightly higher than rolling alone after solution treatment. The limited improvement suggests that Sr ties up part of the aluminium into stable Al-Sr intermetallics, reducing the solute available for conventional Mg-Al precipitation strengthening. For AE44, as-cast rolling to around 13% strain followed by ageing produced hardness of approximately 51 HV, which was close to rolling alone. Thus, ageing had a weaker effect in AE44 than in AZ91 or AJ63.

3 DISCUSSION

4.1 Solution Treatment and Secondary-Phase Stability

The weak effect of solution treatment on hardness reflects the balance between phase dissolution, solute strengthening and possible grain growth. In AZ91, partial dissolution of beta-Mg17Al12 at 410 °C can reduce the volume fraction of hard boundary phases while increasing aluminium supersaturation in the alpha-Mg matrix [5, 13-14]. The net result in this dataset was almost unchanged hardness. The AZ91 micrographs (Figure 3) show that the solutionised condition retained visible heterogeneity, consistent with incomplete homogenisation or the persistence of phase networks at this scale.

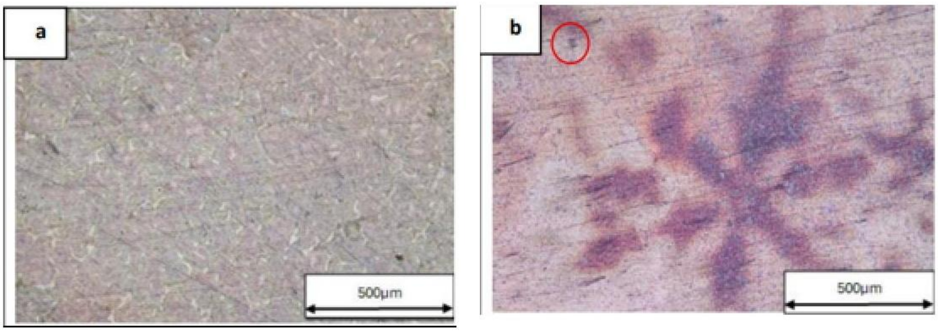

Figure 3 Optical Micrographs of AZ91: (a) As-Cast Microstructure and (b) Solutionised Microstructure. Scale Bars: 500 µm

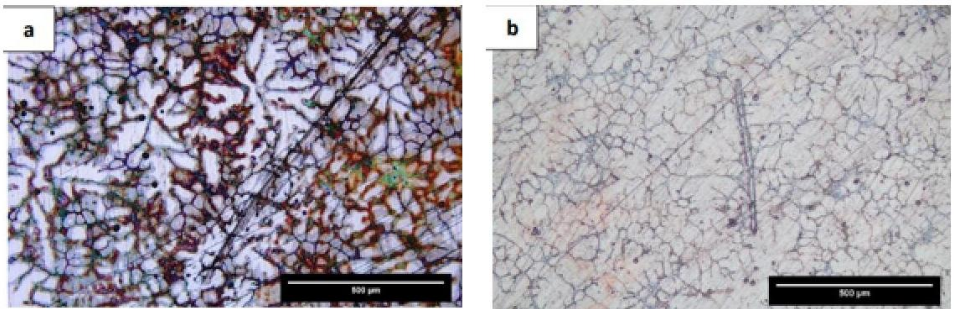

Figure 4 Optical Micrographs of AJ63: (a) As-Cast Microstructure and (b) Solutionised Microstructure. Scale Bars: 500 µm

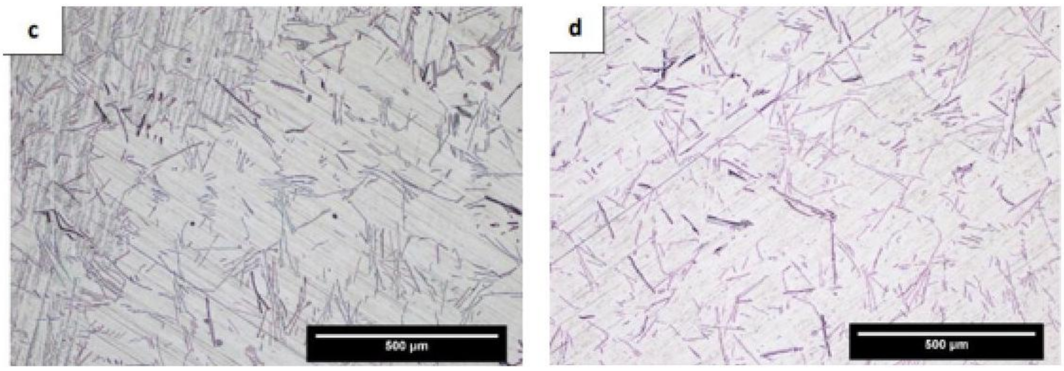

Figure 5 Optical Micrographs of AE44: (a) As-Cast Microstructure and (b) Solutionised Microstructure. Scale Bars: 500 µm

In AJ63, the hardness after solution treatment remained statistically unchanged, but the subsequent rolling behaviour improved markedly. This suggests that solutionising modified matrix condition and phase connectivity more than it changed bulk hardness. Mg-Al-Sr alloys are known to contain stable Sr-bearing intermetallics such as Al4Sr/(Al,Mg)4Sr and ternary phases [8-9]. These phases do not readily dissolve during the applied treatment, but the heat treatment may reduce local stress concentration and interrupt brittle networks (Figure 4-5).

AE44 showed a slight hardness decrease after solution treatment. This is consistent with the high thermal stability of Al-RE intermetallics in Mg-Al-RE alloys [10-12]. If these phases remain largely undissolved, solution treatment does not generate enough supersaturated solute to enable strong subsequent precipitation hardening. Any reduction in hardness can then be attributed to recovery, grain growth or reduced defect density (Figure 6).

4.2 Composition-Dependent Rolling Response

The rolling results can be interpreted through the competition between dislocation multiplication, particle-dislocation interactions, microcracking and recovery. In general, strain hardening is associated with increasing dislocation density, commonly described by the Taylor relation: Delta sigma = M alpha G b sqrt(rho), where M is the Taylor factor, alpha is a constant, G is the shear modulus, b is the Burgers vector and rho is the dislocation density. Hardness is often approximately proportional to yield strength, so increasing dislocation density should increase hardness when damage and recovery are limited [15-17].

As-cast AZ91 hardened strongly at low strain because the beta-Mg17Al12 network and deformation-induced dislocations impeded slip. At higher rolling strain, however, the same brittle network may fragment and localise strain, reducing the apparent hardness benefit. Recent work on rolled AZ91 also reports strong sensitivity of microstructure, texture and mechanical behaviour to rolling reduction [6]. This explains why AZ91 has an optimum strain range instead of a monotonic increase.

AJ63 cracked during direct rolling because its as-cast Al-Sr phase network is more brittle and less tolerant of plastic strain. The sharp decrease in hardness at low strain is therefore interpreted as damage-dominated behaviour rather than true softening of the matrix. After solution treatment, matrix recovery and partial interruption of the phase network improved deformation compatibility, allowing work hardening to dominate up to 8-10% strain. AE44, by contrast, contains more dispersed and thermally stable Al-RE phases that act as obstacles to dislocation motion without the same immediate brittle-network failure. This supports a more continuous hardness increase during rolling [18-25].

4.3 Ageing Response and Strain-Assisted Precipitation

The ageing response followed the sequence AZ91 > AJ63 > AE44. AZ91 contains the highest aluminium content among the three alloys, and its strengthening during ageing is associated with beta-phase precipitation from a supersaturated alpha-Mg matrix [3, 5, 14]. Pre-rolling increased the number of dislocations and defect sites, which can accelerate nucleation and refine precipitate distribution. This explains why solutionising + rolling + ageing achieved the highest hardness in this study. Similar strengthening effects of pre-deformation before ageing have been reported in Mg-Al alloys [7].

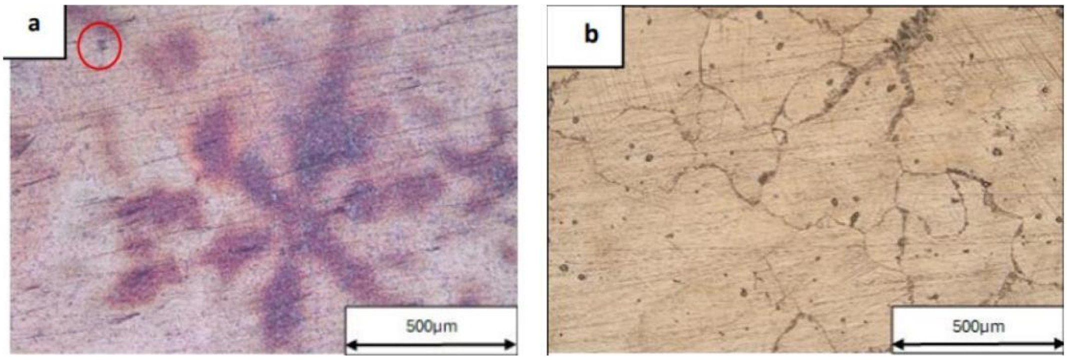

Figure 6 Optical Micrographs of AZ91: (a) Solutionised Condition and (b) Aged Condition After 18 h at 175 °C with Prior Rolling Deformation. Scale Bars: 500 μm

The moderate response of AJ63 is attributed to aluminium consumption by stable Al-Sr intermetallics, which limits the amount of aluminium available for beta-phase precipitation. AE44 had the weakest ageing response because rare-earth elements form thermally stable Al-RE phases. These phases are beneficial for thermal stability and creep resistance, but they reduce the solute reservoir for conventional age hardening at 175 °C [10-13]. Therefore, in AE44 the dominant strengthening contribution in the present process was rolling-induced dislocation hardening rather than precipitation hardening.

4.4 Processing Route Selection and Limitations

The optimum processing routes identified from the available data are summarised in Table 3. For AZ91, the maximum hardness was obtained by solutionising, rolling to 15% strain and ageing at 175 °C for 18 h. For applications where a simpler process is preferred, direct rolling of the as-cast alloy within the optimum strain range can still produce a substantial hardness increase. For AJ63, direct rolling of the as-cast alloy should be avoided because cracking dominates the response. Solution treatment before rolling is necessary. For AE44, solution treatment alone is not useful for hardness improvement; controlled rolling in the as-cast condition is a more efficient route.

Table 3 Recommended Processing Routes for the Investigated Alloys Based on Hardness Response and Cracking Behaviour

Alloy	Recommended route	Peak hardness in this dataset	Main reason	Alloy
AZ91	Solutionising at 410 °C/24 h + 15% rolling + ageing at 175 °C/18 h	~82.4 HV	Strong strain-ageing synergy and beta-phase precipitation	AZ91
AJ63	Solutionising + 8-10% rolling + ageing at 175 °C/18 h	~63 HV	Solutionising improves deformability; ageing response is moderate	AJ63
AE44	Direct as-cast rolling to ~13% strain; ageing optional	~50-51 HV	Al-RE phases are stable; rolling contributes more than ageing	AE44

4 CONCLUSIONS

Solution treatment at 410 °C for 24 h did not significantly increase the hardness of AZ91, AJ63 or AE44, and the differences between the as-cast and solutionised states were statistically insignificant. Among the three alloys, AZ91 showed the strongest overall strengthening response: the highest hardness, approximately 82.4 HV, was obtained after solutionising, 15% rolling and ageing at 175 °C for 18 h, indicating a clear synergistic effect between deformation-induced defects and ageing precipitation. AJ63 could not be effectively rolled in the as-cast condition because brittle cracking dominated its deformation response; therefore, solution treatment before rolling is necessary to improve deformability and enable moderate work hardening and ageing strengthening. AE44 benefited little from solution treatment and ageing, and its hardness improvement mainly resulted from rolling deformation, reaching approximately 50-51 HV at around 13% strain. Overall, the different processing responses are controlled by alloy composition and secondary-phase stability: beta-Mg17Al12 contributes to strong age hardening in AZ91, Al-Sr networks increase the cracking sensitivity of AJ63, and stable Al-RE phases limit the ageing response of AE44. Future work should combine hardness testing with tensile testing, EBSD texture analysis and SEM/EDS phase characterisation to validate the proposed mechanisms and further optimise the processing windows for each alloy.

COMPETING INTERESTS

The authors have no relevant financial or non-financial interests to disclose.

REFERENCES

[1] Liu B, Yang J, Zhang X, et al. Development and application of magnesium alloy parts for automotive OEMs: A review. Journal of Magnesium and Alloys, 2023, 11(1): 15-47. DOI: 10.1016/j.jma.2022.12.015.
[2] Mordike B L, Ebert T. Magnesium: Properties - applications - potential. Materials Science and Engineering A, 2001, 302(1): 37-45. DOI: 10.1016/S0921-5093(00)01351-4.
[3] Nie J F. Precipitation and hardening in magnesium alloys. Metallurgical and Materials Transactions A, 2012, 43: 3891-3939. DOI: 10.1007/s11661-012-1217-2.
[4] Shi Z Z, Chen H T, Zhang K, et al. Crystallography of precipitates in Mg alloys. Journal of Magnesium and Alloys, 2021, 9(2): 416-431. DOI: 10.1016/j.jma.2020.06.013.
[5] Alomairy S. Dissolution mechanism and kinetics of beta-Mg17Al12 phases in AZ91 magnesium alloy. Journal of Magnesium and Alloys, 2024, 12(4): 1581-1592. DOI: 10.1016/j.jma.2024.03.020.
[6] Tolouie E, Jamaati R. Effect of rolling reduction on the microstructure, texture, and mechanical behavior of AZ91 alloy. Journal of Materials Research and Technology, 2023, 26: 7947-7957. DOI: 10.1016/j.jmrt.2023.09.119.
[7] Liu F, Xin R, Zhong Y, et al. Effect of cold rolling on aging precipitation and mechanical properties of magnesium-aluminum alloy. Journal of Magnesium and Alloys, 2025, 13(6): 2606-2617. DOI: 10.1016/j.jma.2023.06.015.
[8] Aljarrah M, Parvez M A, Li J, et al. Microstructural characterization of Mg-Al-Sr alloys. Science and Technology of Advanced Materials, 2007, 8(4): 237-248. DOI: 10.1016/j.stam.2007.01.003.
[9] Rzychoń T, Kiełbus A, Dercz G. Structure refinement of the multi-phase Mg-Al-Sr alloy. Solid State Phenomena, 2010, 163: 169-172. DOI: 10.4028/www.scientific.net/SSP.163.169.
[10] Zhang T T, Yu W B, Ma C S, et al. The effect of different high pressure die casting parameters on 3D microstructure and mechanical properties of AE44 magnesium alloy. Journal of Magnesium and Alloys, 2023, 11(9): 3141-3150. DOI: 10.1016/j.jma.2022.05.001.
[11] Rzychoń T, Kiełbus A. Microstructural stability and creep properties of die casting Mg-4Al-4RE magnesium alloy. Materials Characterization, 2009, 60(10): 1107-1113. DOI: 10.1016/j.matchar.2009.05.014.
[12] Zhu S, Easton M A, Abbott T B, et al. The influence of individual rare earth elements (La, Ce, or Nd) on creep resistance of die-cast magnesium alloy AE44. Advanced Engineering Materials, 2016, 18(6): 932-937. DOI: 10.1002/adem.201500545.
[13] Chia T L, Easton M A, Zhu S M, et al. The effect of alloy composition on the microstructure and tensile properties of binary Mg-rare earth alloys. Intermetallics, 2009, 17(7): 481-490. DOI: 10.1016/j.intermet.2008.12.009.
[14] Clark J B. Age hardening in a Mg-9 wt.% Al alloy. Acta Metallurgica, 1968, 16(2): 141-152. DOI: 10.1016/0001-6160(68)90106-8.

[15] Esgandari B A, Nami B, Miresmaeili S M, et al. The effect of Ca and RE elements on the precipitation kinetics of AZ91 magnesium alloy. Materials Science and Engineering A, 2011, 528(15): 5018-5024. DOI: 10.1016/j.msea.2011.03.045.
[16] Bailey J E, Hirsch P B. The dislocation distribution, flow stress, and stored energy in cold-worked polycrystalline silver. Philosophical Magazine, 1960, 5(53): 485-497. DOI: 10.1080/14786436008238300.
[17] Ashby M F. The deformation of plastically non-homogeneous materials. Philosophical Magazine, 1966, 14(132): 1157-1178. DOI: 10.1080/14786436608224282.
[18] Armstrong R W. Hall-Petch relationship: Use in characterizing properties of aluminum and aluminum alloys. Materials Science and Engineering A, 2014, 607: 14-19. DOI: 10.1016/j.msea.2014.03.099.
[19] Rokhlin L L. Magnesium Alloys Containing Rare Earth Metals: Structure and Properties. London: Taylor & Francis, 2003.
[20] Asgari A, Delavar H, Sedighi M. Microstructure and surface integrity of machined AZ91 magnesium alloy. Journal of Materials Research and Technology, 2023, 22: 735-746. DOI: 10.1016/j.jmrt.2022.11.006.
[21] Li Y, Gao Y, Zhang X, et al. Microstructure and mechanical properties of Mg-Al-La-Mn composites reinforced by AlN particles. Materials, 2024, 17(14): 3497. DOI: 10.3390/ma17143497.
[22] Wu G, Wang C, Sun M, et al. Recent developments and applications on high-performance cast magnesium rare-earth alloys. Journal of Magnesium and Alloys, 2021, 9(1): 1-20. DOI: 10.1016/j.jma.2020.06.021.
[23] Xie J, Zhang J, You Z, et al. Towards developing Mg alloys with simultaneously improved strength and corrosion resistance via RE alloying. Journal of Magnesium and Alloys, 2021, 9(1): 41-56. DOI: 10.1016/j.jma.2020.08.016.
[24] Tekumalla S, Gupta M. Mechanical properties of magnesium-rare earth alloy systems: A review. Metals, 2015, 5(1): 1-39. DOI: 10.3390/met5010001.
[25] Kiełbus A. Microstructure and properties of casting magnesium alloys designed to work in elevated temperature. In: Magnesium Alloys: Selected Issue. IntechOpen, 2018. DOI: 10.5772/intechopen.80291.